

## Electronic Supplementary Information

# **Layered supramolecular network of cyclodextrin triplet with azobenzene-grafting polyoxometalate for dye degradation and partner-enhancement**

Bo Gao, Bao Li\* and Lixin Wu\*

State Key Laboratory of Supramolecular Structure and Materials  
College of Chemistry, Jilin University  
Changchun 130012, P.R. China  
E-mail: wulx@jlu.edu.cn; libao@jlu.edu.cn

## Table of contents

Materials .....	2
Measurements .....	2
Synthesis of host tri-CD .....	2
Synthesis of guest POMs .....	3
Preparation of supramolecular network assembly .....	4
Characterizations of tri-CD and supramolecular network assembly .....	4
Dyes' degradation by supramolecular network assembly .....	11
References.....	24

## Materials.

Cationic dyes, rhodamine B (RhB), malachite green (MG), cationic acriflavine (AC) are the products of Aladdin Chemistry Co., Ltd. Anionic dyes, fluorescein sodium (FS) and eosin Y (EY), are the products of Sinopharm Chemical Reagent Co., Ltd. Cationic methylene blue (MB) is sourced from Tianjin Guangfu Fine Chemical Reagent Institute. The remaining chemicals and solvents are purchased from Beijing Chemical Reagent Industry. Water used in our work is deionized water. The 1,3,5-triethynylbenzene, mono-6-N<sub>3</sub>- $\beta$ -CD, azo-MnMo<sub>6</sub>, and azo-AlMo<sub>6</sub> are synthesized according to previous publications.<sup>1-4</sup>

## Measurements.

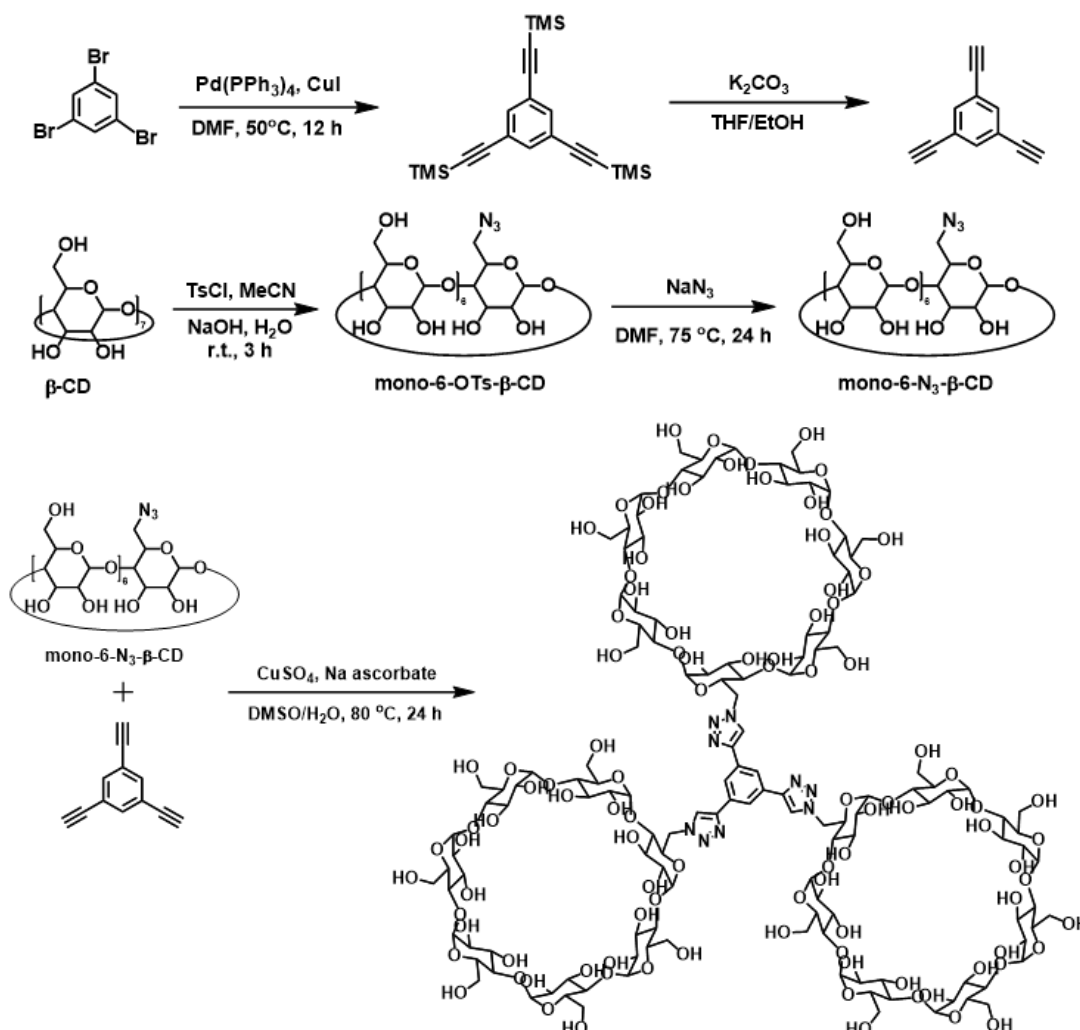
The UV-Vis spectra are taken on a spectrophotometer (Varian CARY 50 Probe). <sup>1</sup>H NMR, <sup>13</sup>C NMR and 2D NOESY NMR spectra are recorded on a Bruker AVANCE 500 MHz spectrometer. The chemical shifts are referenced to the solvent values ( $\delta$  = 2.50 ppm for DMSO-*d*<sub>6</sub> and  $\delta$  = 4.79 ppm for D<sub>2</sub>O). Matrix-assisted laser desorption / ionization time-of-flight mass spectrum (MALDI-TOF) is recorded on a Bruker autoflex MALDI-TOF/TOF mass spectrometer equipped with a nitrogen laser (337 nm, 3 ns pulse), operating in the positive ion reflector mode with a detector potential of -4.75 kV. X-ray diffraction (XRD) data are collected on a Rigaku X-ray diffractometer using Cu K $\alpha$  radiation at a wavelength of 1.542 Å. Transmission electron microscopy (TEM) is conducted on a JEOL JEM 2010 under an accelerating voltage of 200 kV without staining. Atomic force microscope (AFM) images are taken with a Bruker Dimension FastScan under ambient conditions, operating on the tapping mode with an optical readout using Si cantilevers. Organic elemental analysis (C, H, and N) is performed on a Vario micro cube from Elementar company, while inorganic elemental analysis (Mn, Al, Mo and Na) is performed on an iCAP 7000 inductively coupled plasma atomic emission spectrometer (ICP-AES). Liquid chromatography mass spectrometry (LC-MS) is obtained on a Quattro Premier UPLC-MS. Dynamic light scattering (DLS) measurements are performed by using a Malvern Zetasizer Nano-ZS instrument at room temperature. Isothermal titration calorimetric (ITC) data are collected on a Micro Cal VP-isothermal titration calorimeter from Malvern.

## Synthesis of host tri-CD.

Tri-CD is synthesized following the route shown in Scheme S1 by referring to a similar method to the one in our previous studies,<sup>5</sup> Typically, CuSO<sub>4</sub>·5H<sub>2</sub>O (3.4 mmol, 0.85 g) is dispersed in 50 mL of DMSO containing 1,3,5-triethynylbenzene (1.0 mmol, 0.15 g) and mono-6-N<sub>3</sub>- $\beta$ -CD (3.4 mmol, 3.9 g) which is prepared following the published procedures. Then, sodium ascorbate solution (6.8 mmol, 1.3 g) in 10 mL of water is added under stirring. The solution is then heated to 80°C for 24 hours and then pours into acetone after being cooled down. The formed precipitates are collected by filtration and then purified over a silica-gel chromatography with *i*-propanol/H<sub>2</sub>O/NH<sub>3</sub>·H<sub>2</sub>O at volume ratio of 80:15:5 to 60:35:5 as the eluents, giving the pure tri-CD (0.8 g) product as a brown solid in a yield of 22%.

<sup>1</sup>H NMR (500 MHz; D<sub>2</sub>O, 25 °C,  $\delta$ ): 8.54 (s, 3H, Ar-H), 8.27 (s, 3H, Ar-H), 5.26 (s, 3H, CH<sub>2</sub>), 5.19-5.04 (m, 21H, CD), 4.97 (s, 3H, CH<sub>2</sub>), 5.25-3.45 (m, 141H, CD), 3.20 (d, 3H, CH<sub>2</sub>) 3.00 (d, 3H, CH<sub>2</sub>). <sup>13</sup>C NMR (101 MHz, DMSO-*d*<sub>6</sub>, 25 °C  $\delta$ ): 146.11, 132.45, 124.46, 121.92, 102.46, 83.41, 82.01, 73.54, 72.87, 72.54, 70.05, 60.43, 59.77, 50.74. Maldi-Tof

MS: calculated  $C_{138}H_{213}N_9O_{102}+Na^+$ : 3652.17, Found 3652.438; calculated  $C_{138}H_{213}N_9O_{102}+K^+$ : 3668.14, found 3668.815. Elemental Analysis: calculated for  $C_{138}H_{213}N_9O_{102}$ : C, 45.66; H, 5.91; N, 3.47, found: C, 45.24; H, 6.02; N, 3.51.



Scheme S1. The synthetic route of tri-CD.

### Synthesis of guest POMs.

The azo- $AlMo_6$  and azo<sub>2</sub>- $MnMo_6$  are prepared according to previous publications.<sup>3-4</sup>

azo- $AlMo_6$ : <sup>1</sup>H NMR (500 MHz, DMSO-*d*<sub>6</sub>, 25 °C, δ): 7.86 (t, 4H, Ar-H), 7.57 (t, 2H, Ar-H), 7.52 (t, H, Ar-H), 7.43 (s, 1H, CONH), 7.09 (d, 2H, Ar-H), 4.68 (s, 4H, CH<sub>2</sub>), 4.53 (s, 2H, CH<sub>2</sub>), 3.68 (s, 3H, OH). Elemental analysis (%): calculated for Na<sub>3</sub>C<sub>18</sub>H<sub>18</sub>O<sub>23</sub>N<sub>3</sub>AlMo<sub>6</sub>(OH)<sub>3</sub>: C 15.82; H 1.55; N 3.07, Al 1.97, Mo 42.11, Na 5.05 found C 15.35; H 1.80; N 3.40, Al 1.84, Mo 41.88, Na 5.23.

azo<sub>2</sub>- $MnMo_6$ : <sup>1</sup>H NMR (500 MHz; D<sub>2</sub>O, 25 °C, δ): 64.10 (br, 12H, CH<sub>2</sub>), 7.94 (d, 4H, Ar-H), 7.86 (d, 4H, Ar-H), 7.63 (m, 6H, Ar-H), 7.22(d, 4H, Ar-H), 5.18 (br, 4H, CH<sub>2</sub>). Elemental analysis (%) calcd. for C<sub>36</sub>H<sub>36</sub>N<sub>6</sub>O<sub>28</sub>Na<sub>3</sub>MnMo<sub>6</sub>: C 25.43, H 2.13, N 4.94, Mn 3.23, Mo 33.86, Na 4.06; found: C 25.02, H 2.24, N 4.75, Mn 3.28, Mo 33.90, Na 4.02.

## Preparation of supramolecular network assembly.

The prepared guest  $\text{azo}_2\text{-MnMo}_6$  (10.5 mg, 6.18  $\mu\text{mol}$ ) and host tri-CD (33.6 mg, 9.26  $\mu\text{mol}$ ) precursors are dissolved in water (10.0 mL). The solution is then encountered a radiation of 366 nm LED light for 6 h so that the azobenzene groups transfer from *trans*- into *cis*-state for the prevention of quick inclusion-induced defects. After that treatment, the mixture solution is allowed to incubate in dark place and the host-guest inclusion occurs gradually accompanying by the turning of *cis*-structure back to *trans*- state. With the water evaporation of the sample solution in an dried atmosphere in the following two weeks, the solid powder of the supramolecular network assembly is obtained.

Elemental analysis (%) of the prepared supramolecular network assembly with a chemical formula of  $[\text{azo}_2\text{-MnMo}_6]_3[\text{tri-CD}]_2$ : calculated for:  $(\text{C}_{36}\text{H}_{36}\text{MnMo}_6\text{N}_6\text{Na}_3\text{O}_{28})_3(\text{C}_{138}\text{H}_{213}\text{N}_9\text{O}_{102})_2 \cdot 50(\text{H}_2\text{O})$ , C, 34.78; H, 4.82; N, 3.80; Mn, 1.24; Mo, 13.02; and Na, 1.56. Found: C, 34.31; H, 5.22; N, 3.36; Mn, 1.20; Mo, 12.95; and Na, 1.51.

Thermal Gravimetric Analysis (TGA): the original molecular weight is 13261, based on the chemical formula calculated from elemental analysis measurement. Suppose the all organic components have been exhausted and residue of metal ions in the form of oxides,  $[\text{MnO}_2(\text{MoO}_3)_6(\text{Na}_2\text{O})_{1.5}]_3$  with the weight 3130, the calculated weight remaining is 23.6%, and found weight remaining is 23.3% after heating to over 700°C at the turning point.

## Characterizations of building units and supramolecular network assembly.

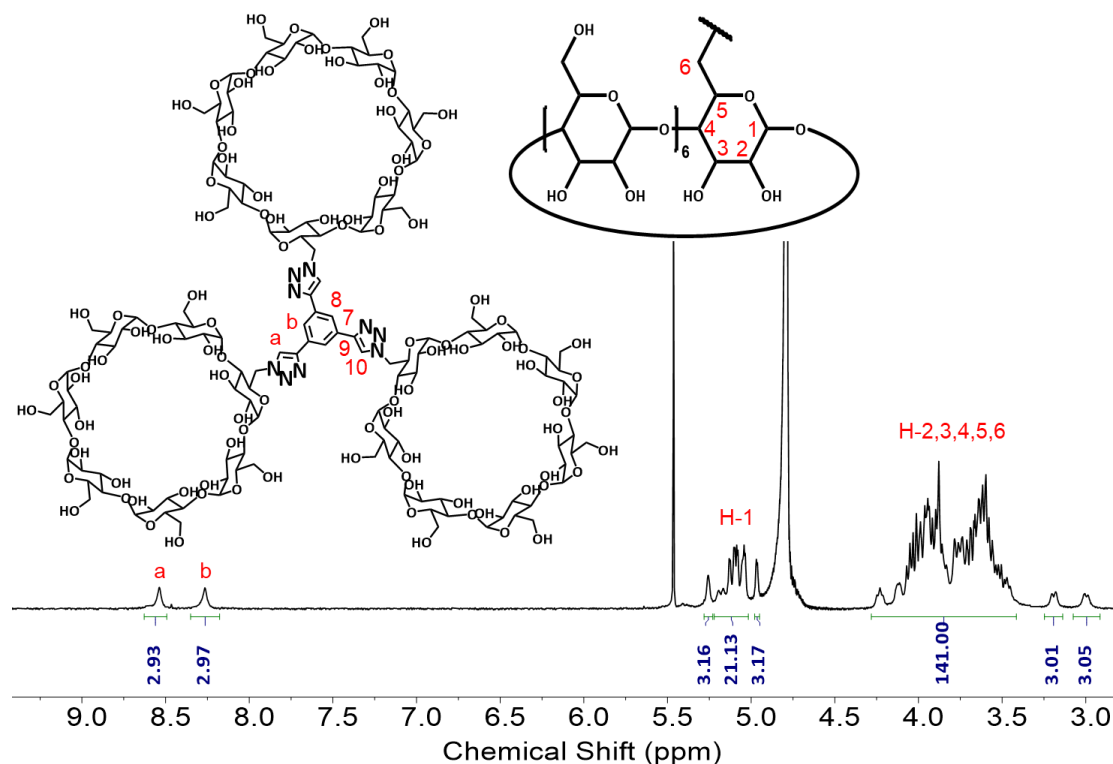
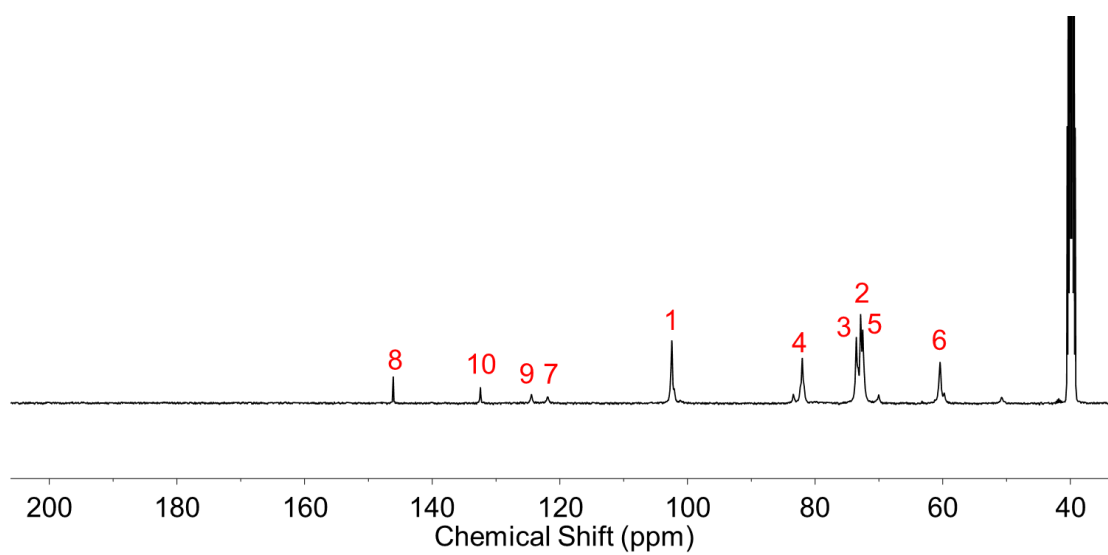
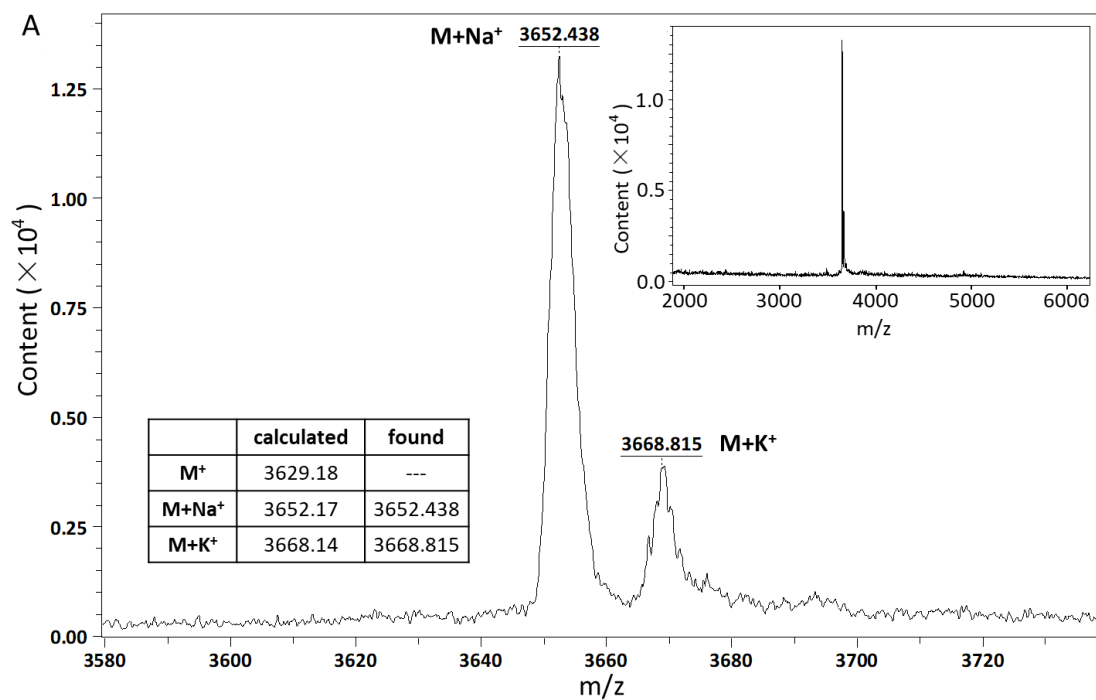
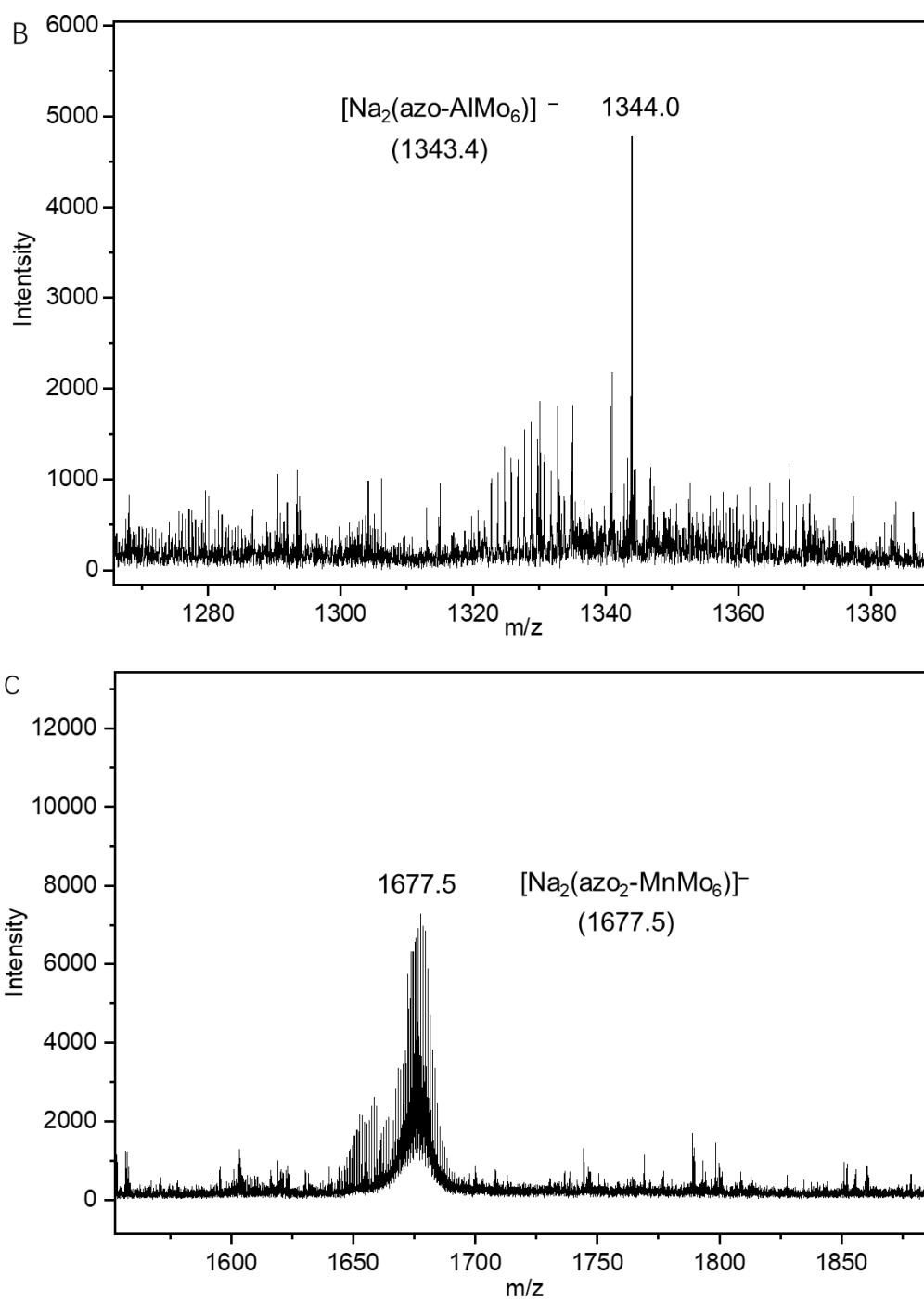


Fig. S1  $^1\text{H}$  NMR spectrum of tri-CD in  $\text{D}_2\text{O}$ .



**Fig. S2**  $^{13}\text{C}$  NMR spectrum of tri-CD in  $\text{DMSO-}d_6$ .





**Fig. S3** Maldi-tof MS spectra of (A) tri-CD, (B) azo- $\text{AlMo}_6$ , and (C)  $\text{azo}_2\text{-MnMo}_6$ .

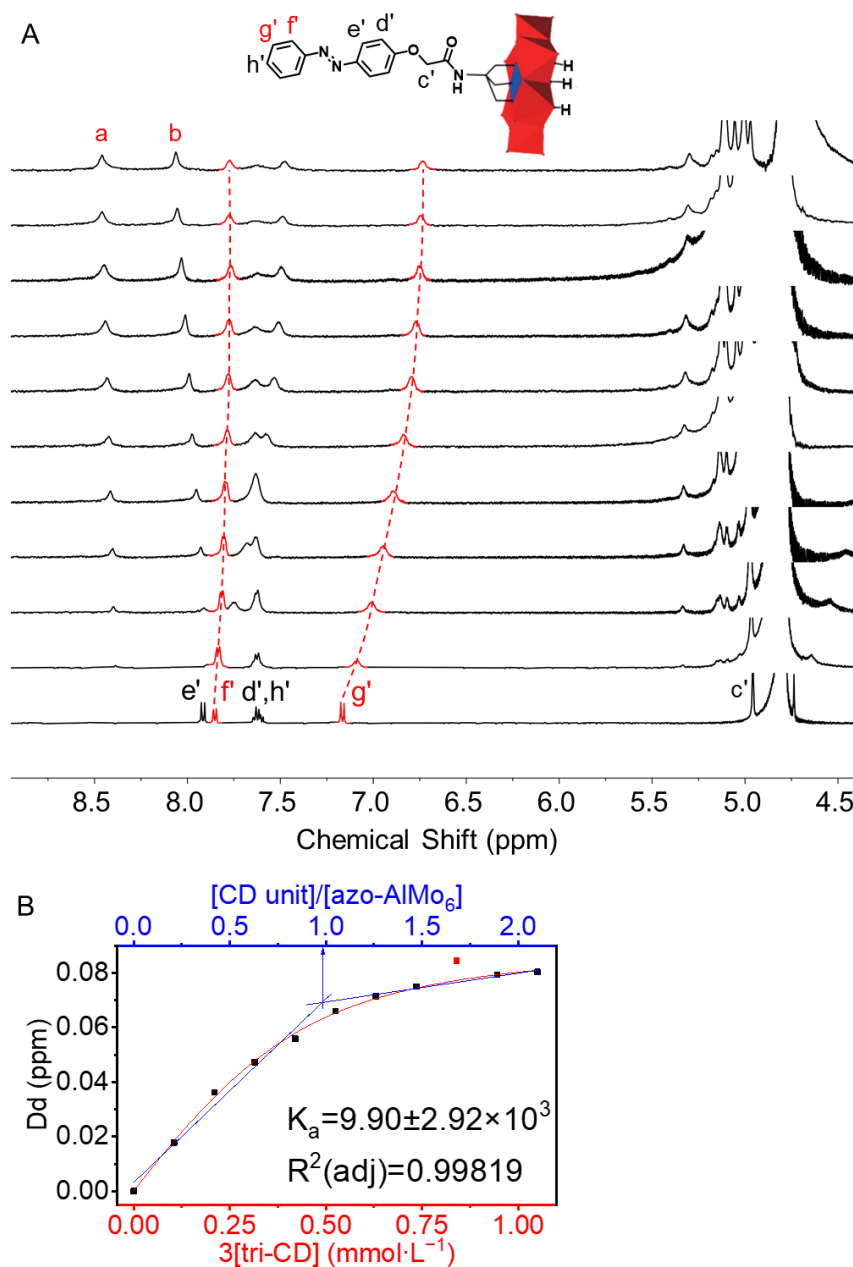


**Fig. S4** (A) NMR titration spectra of the mixture with fixed  $[\text{azo-A1Mo}_6]$  at  $0.5 \text{ mmol}\cdot\text{L}^{-1}$  and changed  $[\text{tri-CD}]$  from 0 to  $0.35 \text{ mmol}\cdot\text{L}^{-1}$  with an interval of  $0.035 \text{ mmol}\cdot\text{L}^{-1}$  from bottom to top, and (B) shifting plots of peak f' versus the concentration increase of tri-CD, and non-linear fitting curve painted red for calculating  $K_a$  corresponds the down red axis and linear fitting for calculating stoichiometric ratio painted blue corresponds the up blue axis.

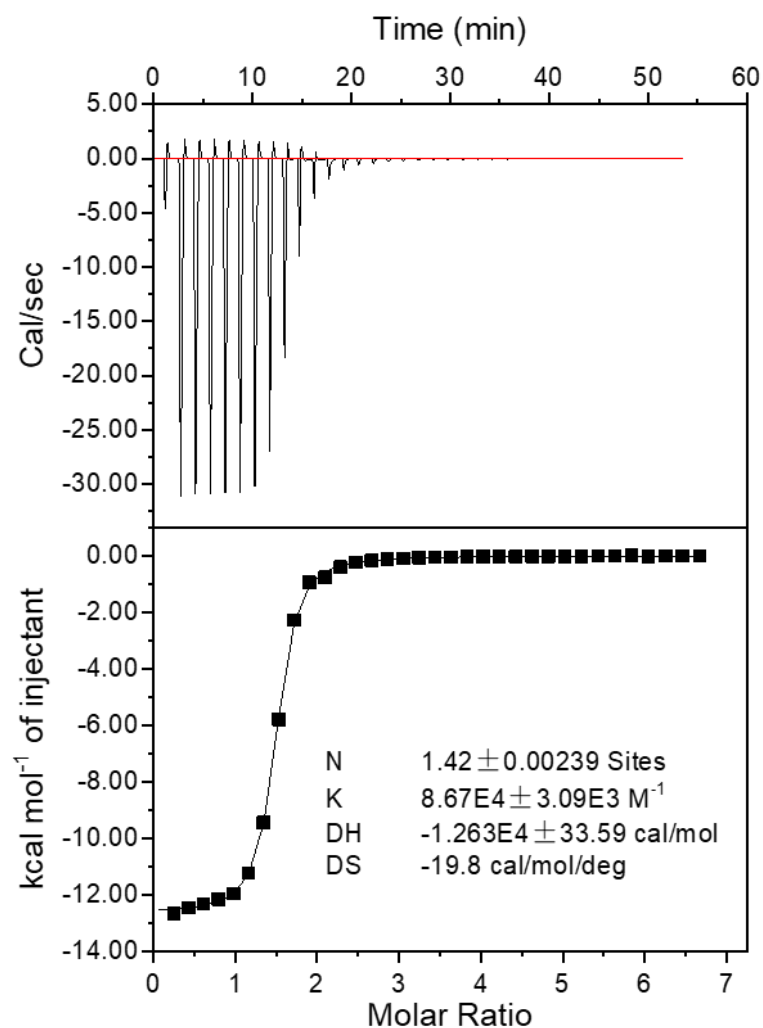


**Fig. S5** ITC curve measured by adding guest azo<sub>2</sub>-MnMo<sub>6</sub> (36.0 mmol·L<sup>-1</sup>) solution into tri-CD solution (1.0 mmol·L<sup>-1</sup>). The given data: binding ratio N is ca. 1.42, binding constant is  $8.67(\pm 0.31) \times 10^3 \text{ mol}^{-1}$ , while  $\Delta H$  is  $-1.26(\pm 33.59) \times 10^4 \text{ cal}\cdot\text{mol}^{-1}$ ,  $\Delta S$  is  $-19.80 \text{ cal}\cdot\text{mol}^{-1}/^\circ\text{C}$ .

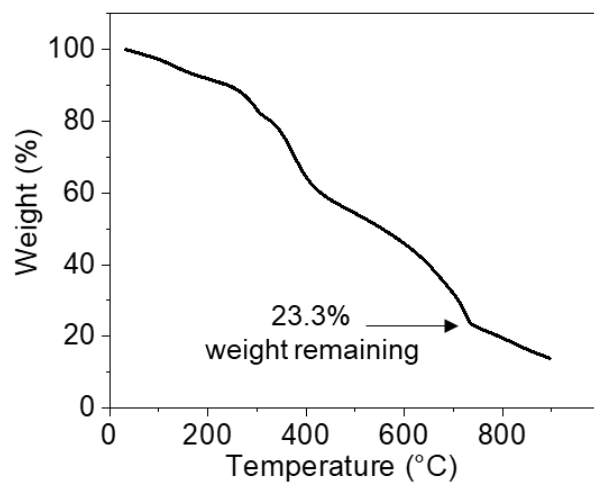


**Fig. S6** TGA curve of the prepared supramolecular porous assembly.

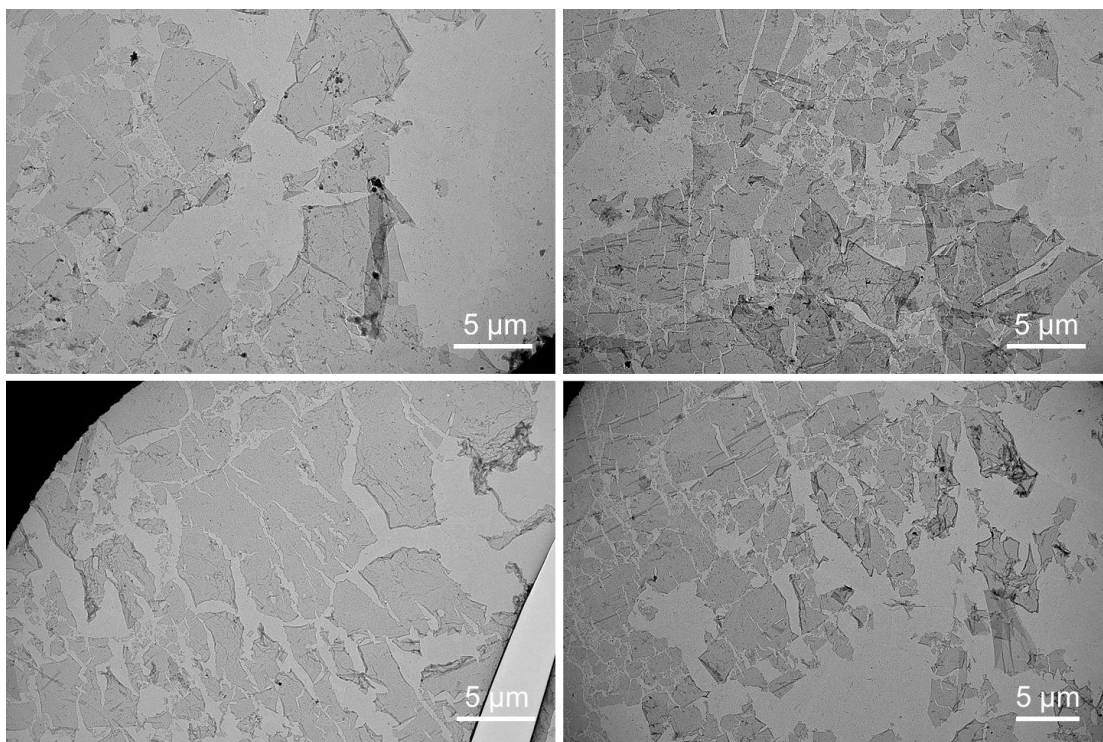


**Fig. S7** TEM images at large scale, prepared by dropping the supramolecular complex aqueous solution on copper grid and then evaporating naturally.

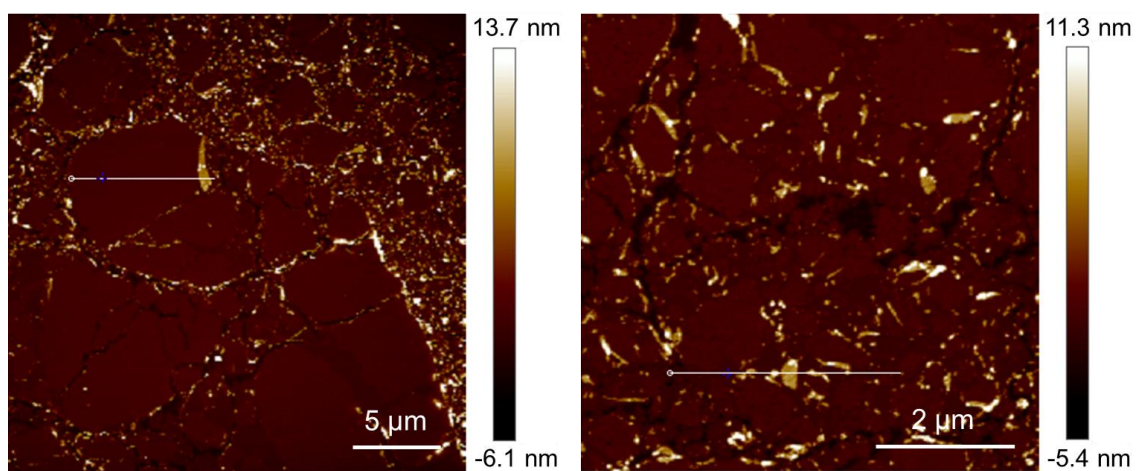


**Fig. S8** AFM images at large scale, prepared by dropping the supramolecular complex aqueous solution on silicon wafer and then evaporating naturally.

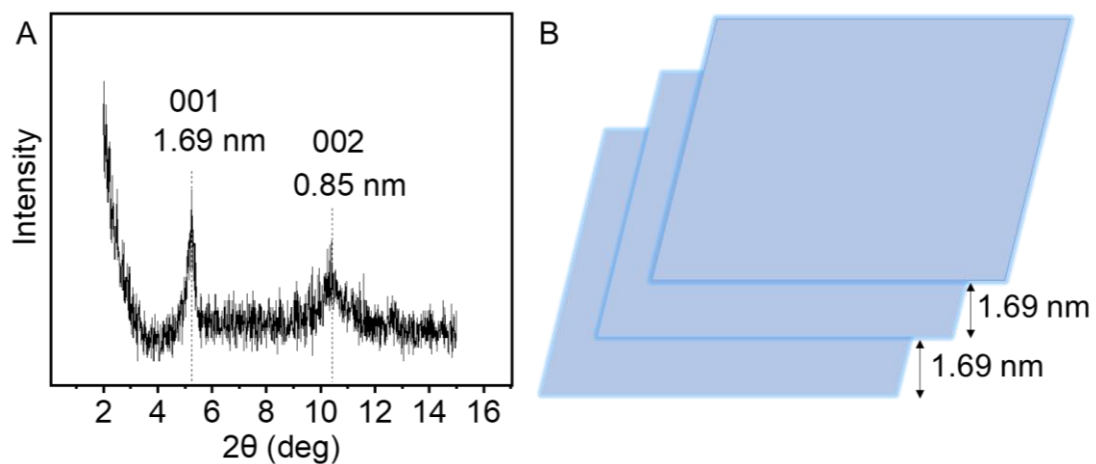


**Fig. S9** (A) Powder XRD spectrum of assembly powder and (B) layered packing model.

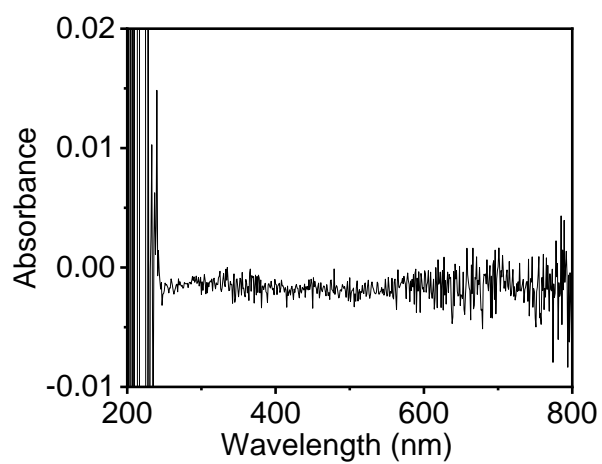


**Fig. S10** UV-vis spectrum of the supramolecular assembly retention in dichloromethane solution, in which the sample is dispersed and stirred for 1 d and then centrifuged to remove the assembly precipitate to detect the solubility of the assembly.

## Dyes' degradation by supramolecular network assembly.

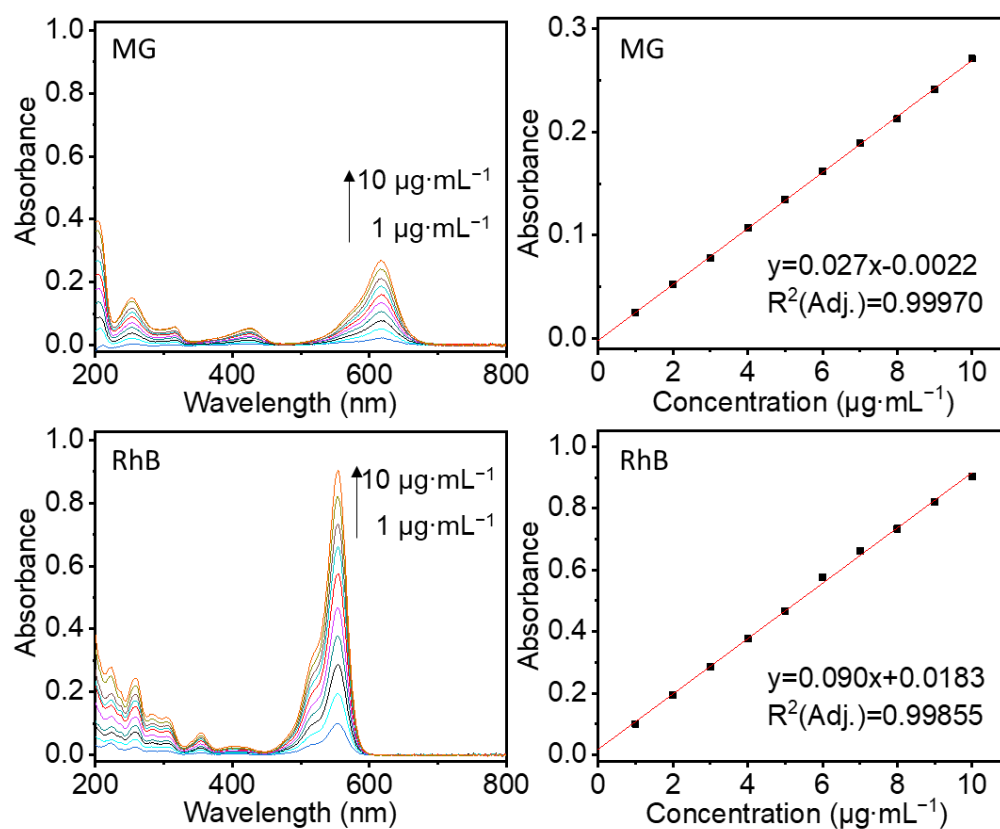


**Fig. S11** UV-vis spectra and corresponding work plots of isolated RhB and MG versus their concentration increase in water.

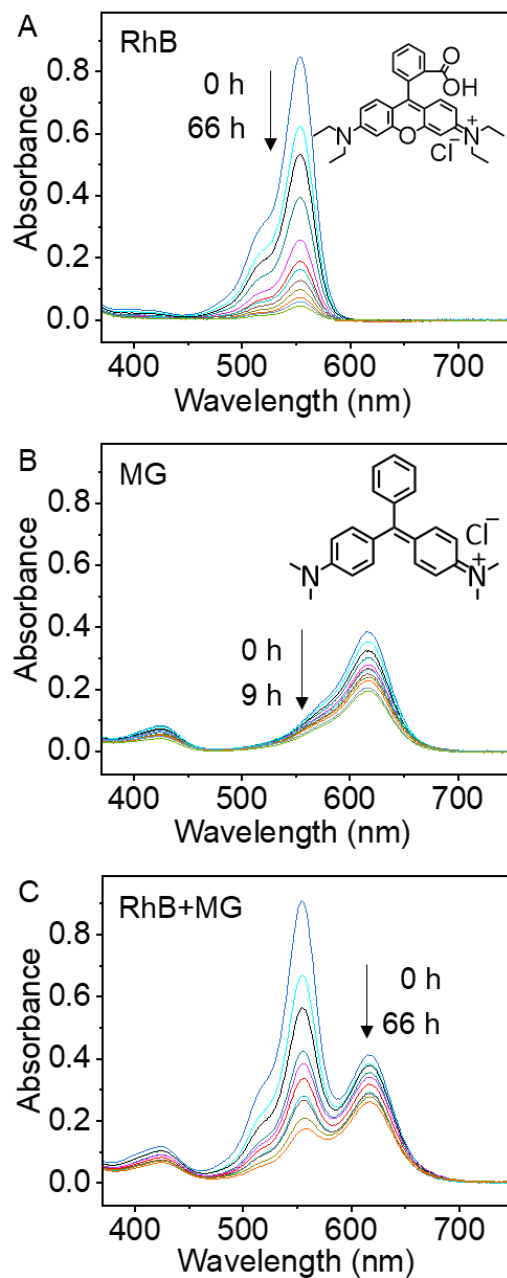


**Fig. S12** UV-vis spectra of (A) RhB, (B) MG and (C) their mixture at 1:1 mass ratio versus the reaction time in aqueous solution at room temperature (25°C) in dark place.

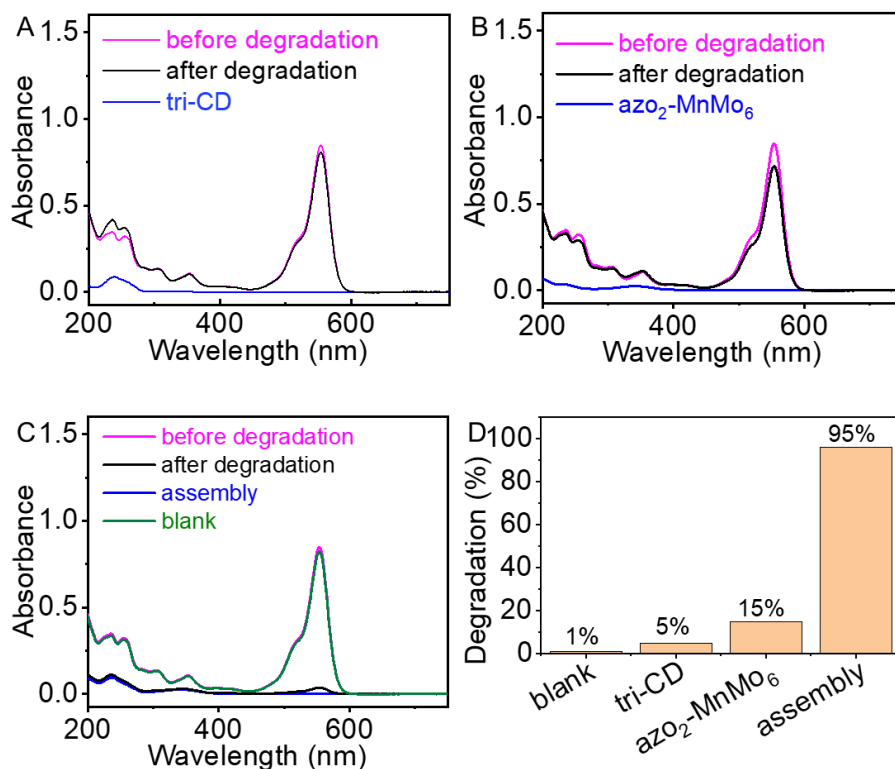


**Fig. S13** UV-vis spectra of RhB aqueous solution in the presence of (A) tri-CD, (B) azo<sub>2</sub>-MnMo<sub>6</sub> and (C) supramolecular assembly before and after 3 days' degradation, and (D) the comparison of the degradation ability under the conditions in (A), (B) and (C).

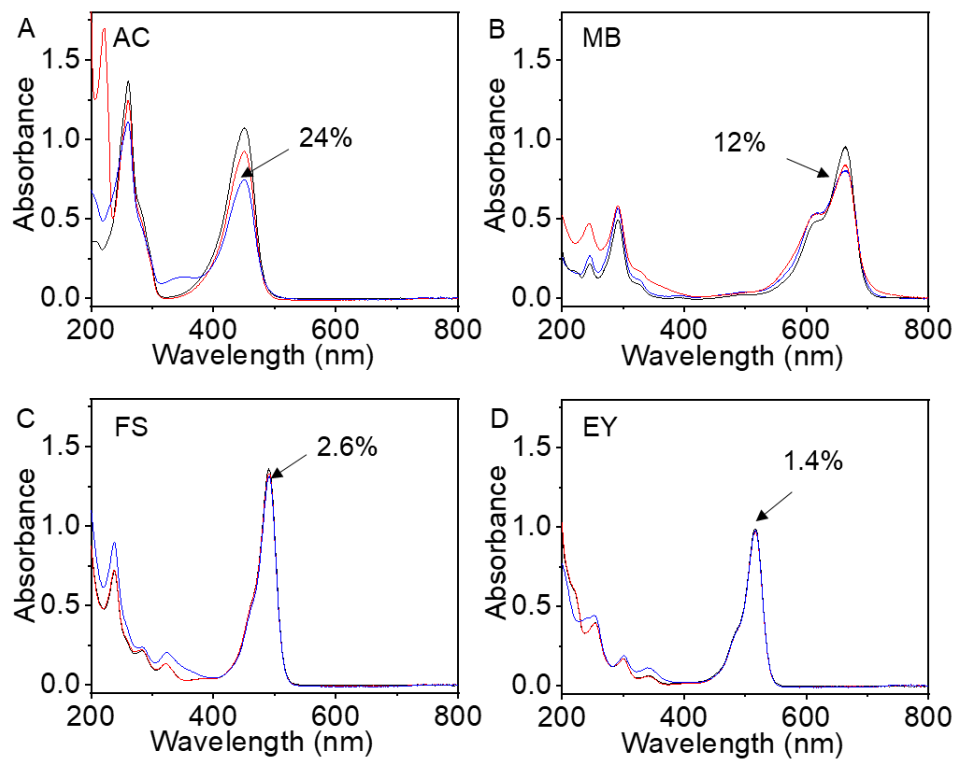


**Fig. S14** UV-vis spectra of individual dyes (A) AC, (B) MB, (C) FS, (D) EY, ( $10 \mu\text{g}\cdot\text{mL}^{-1}$ ) before degradation (black line) and after degradation without (red line) and with the supramolecular assembly (blue line) after 3 days, where the degradation rates are marked.

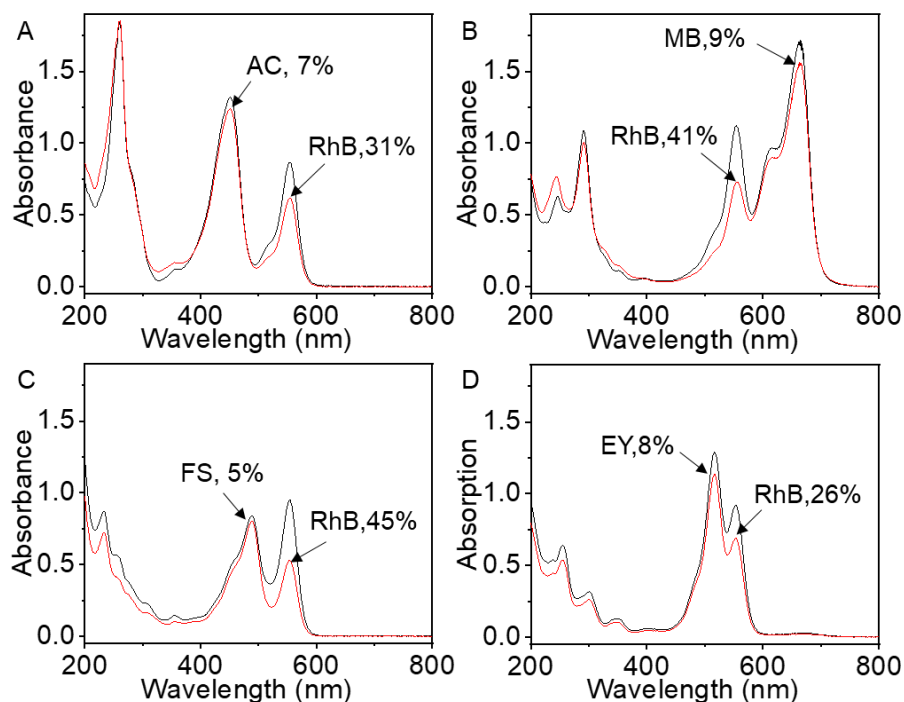


**Fig. S15** UV-vis spectra of RhB in mixed dye aqueous solutions for (A) AC and RhB, (B) MB and RhB, (C) FS and RhB, (D) EY and RhB before degradation (black line) and degradation in the presence of supramolecular assembly (red line) after 9 hours. The concentrations of all four dyes and RhB are  $10 \mu\text{g}\cdot\text{mL}^{-1}$  and the degradation rates are marked.

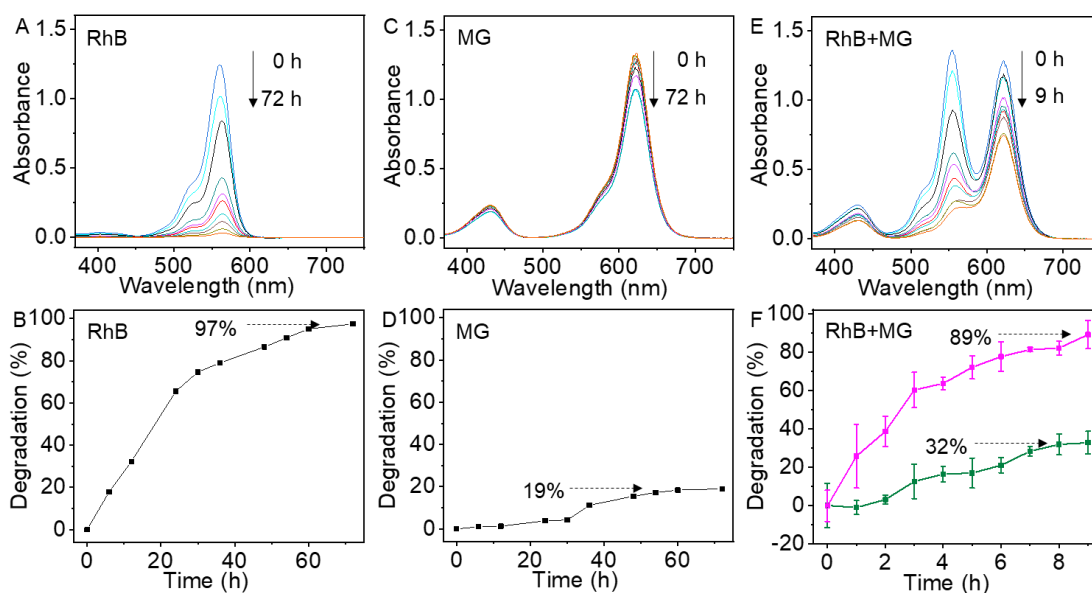


**Fig. 16** UV-vis spectra of (A) RhB, (C) MG and (E) their mixture during degradation in dichloromethane solution versus the time at room temperature in the air, and (B), (D), (F) corresponding dynamic plots of the degradation rates.

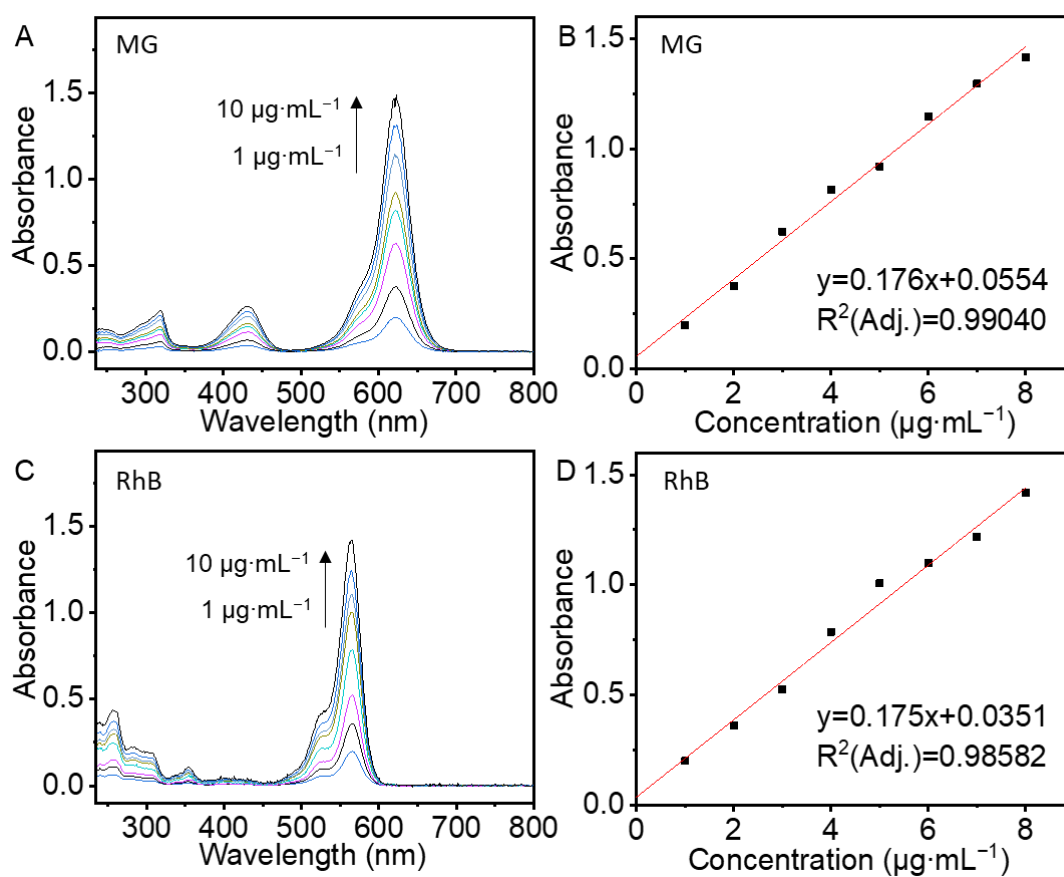


**Fig. S17** UV-vis spectra of RhB and MG in dichloromethane versus the concentration increase and their corresponding work plots.

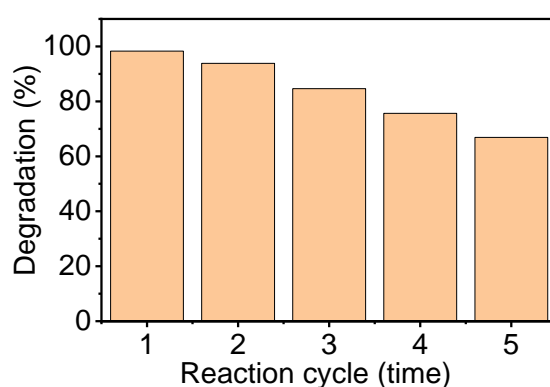


**Fig. S18** Reaction cycles of the dispersed supramolecular assembly powder for the RhB degradation in dichloromethane solution.

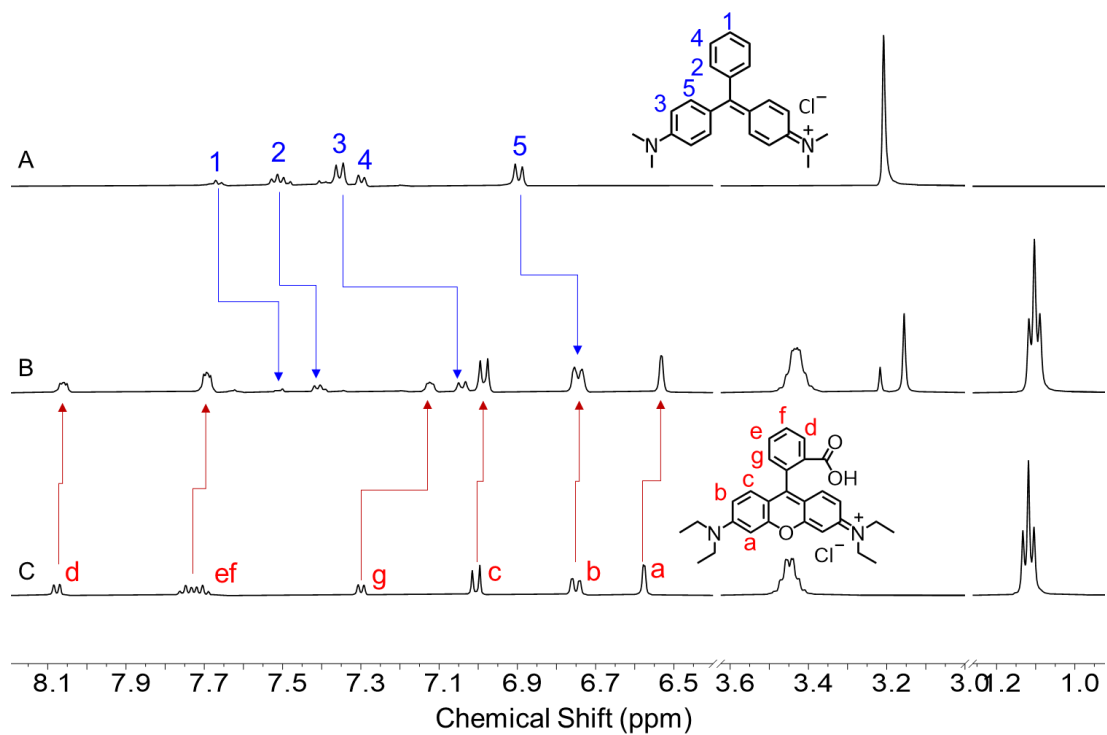


**Fig. S19** <sup>1</sup>H NMR spectra of (A) MG, (B) MG and RhB, and (C) RhB in D<sub>2</sub>O at the concentration of 5.0 mmol·L<sup>-1</sup>.

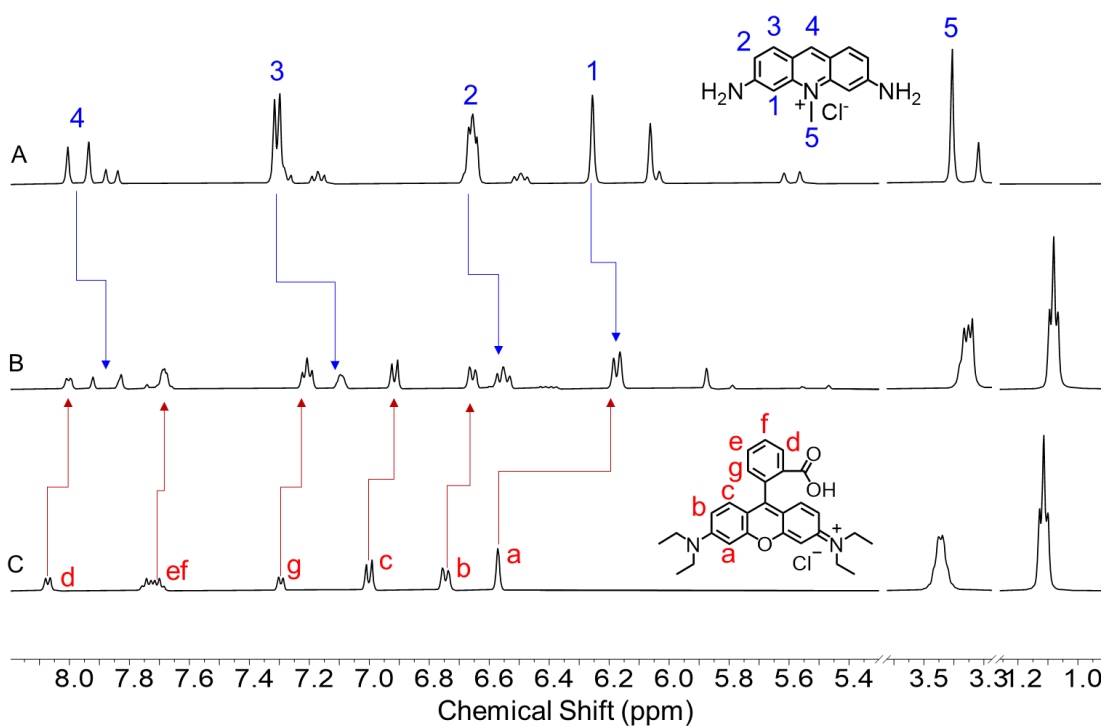


**Fig. S20** <sup>1</sup>H NMR spectra of (A) AC, (B) mixture of AC and RhB, and (C) RhB in D<sub>2</sub>O at the concentration of 5.0 mmol·L<sup>-1</sup>.

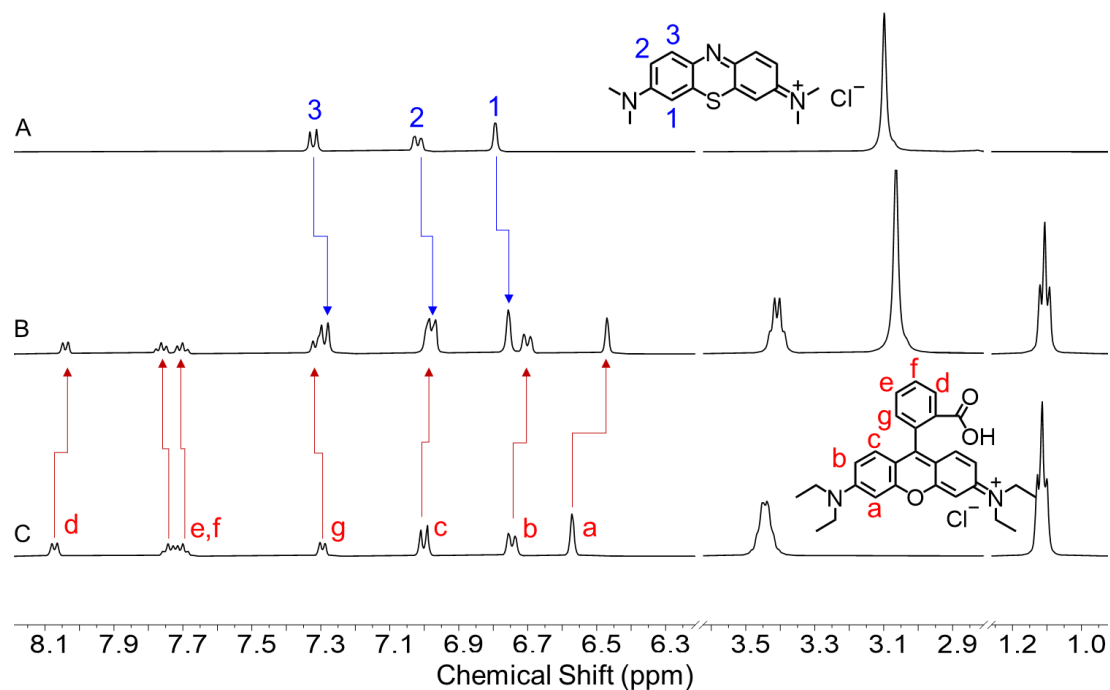


**Fig. S21**  $^1\text{H}$  NMR spectra of (A) MB, (B) mixture of MB and RhB, and (C) RhB in  $\text{D}_2\text{O}$  at the concentration of  $5.0 \text{ mmol}\cdot\text{L}^{-1}$ .

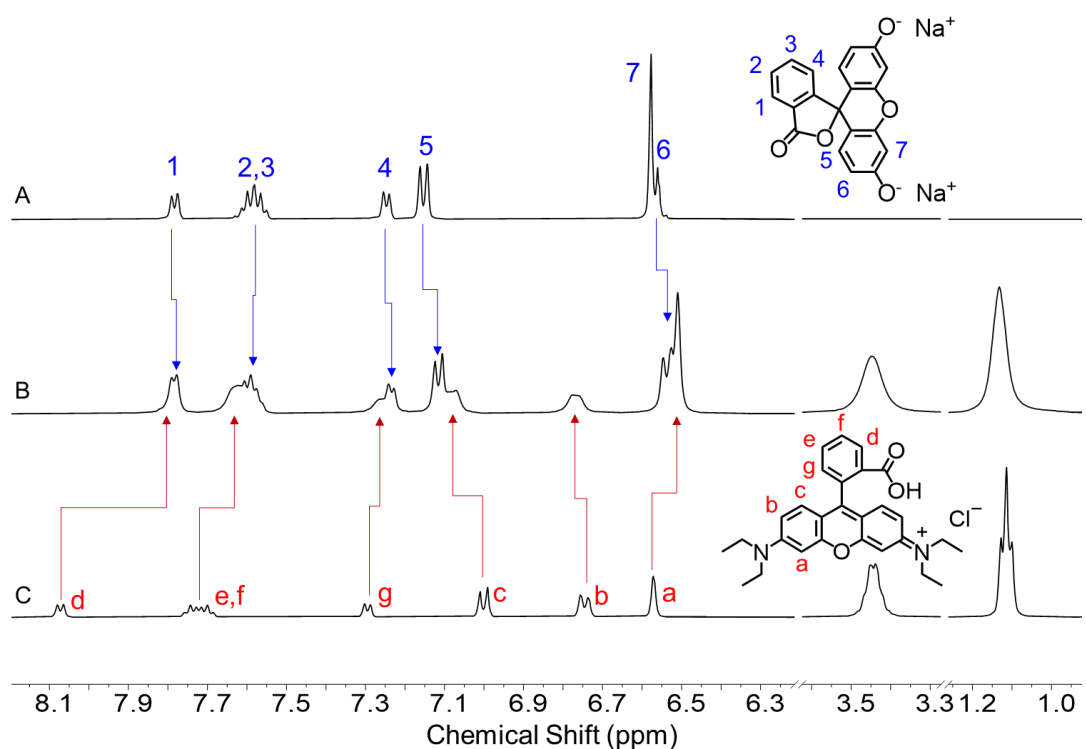


**Fig. S22**  $^1\text{H}$  NMR spectra of (A) FS, (B) mixture of FS and RhB, and (C) RhB in  $\text{D}_2\text{O}$  at the concentration of  $5.0 \text{ mmol}\cdot\text{L}^{-1}$ .

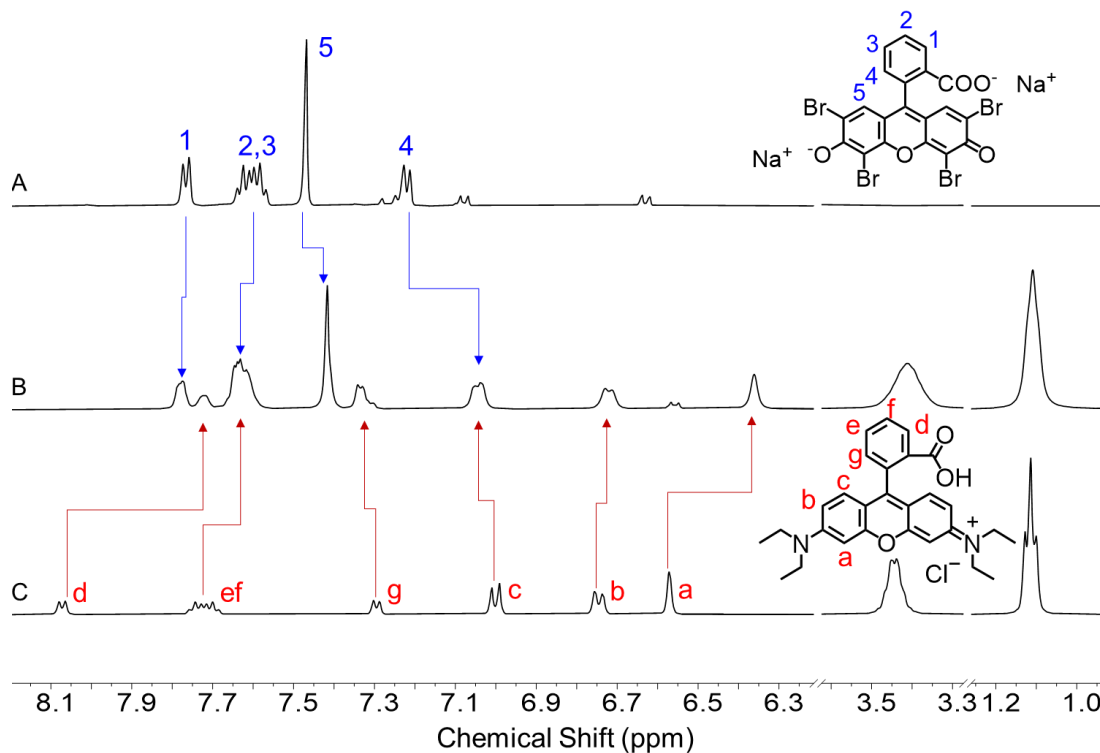


**Fig. S23**  $^1\text{H}$  NMR spectra of (A) EY, (B) mixture of EY and RhB, and (C) RhB in  $\text{D}_2\text{O}$  at the concentration of  $5.0 \text{ mmol}\cdot\text{L}^{-1}$ .

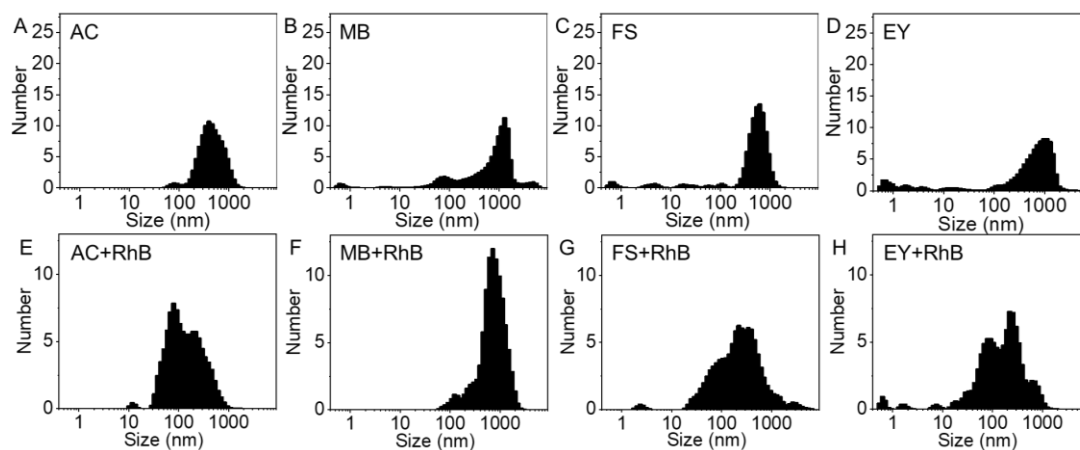


**Fig. S24** DLS diagrams of (A) AC, (B) MB, (C) FS, (D) EY, and the mixtures of RhB with (E) AC, (F) MB, (G) FS, and (H) EY in water, in which the concentrations of all the dyes are set at  $10 \mu\text{g}\cdot\text{mL}^{-1}$ .

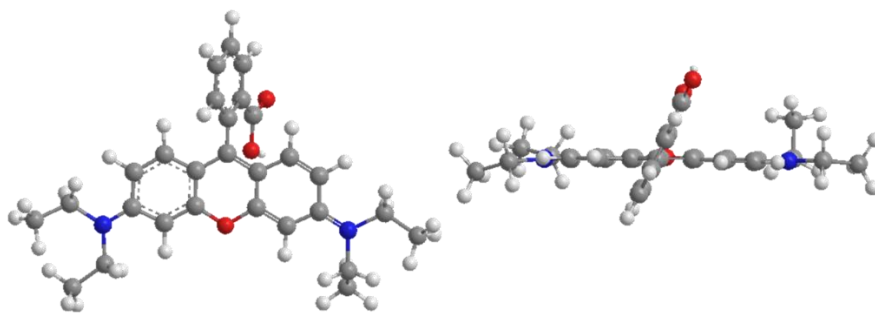


**Fig. S25** Chemical structure of RhB, in which white, grey, red and blue balls are hydrogen, carbon, oxygen and nitrogen atoms, respectively. Counterion is omitted.

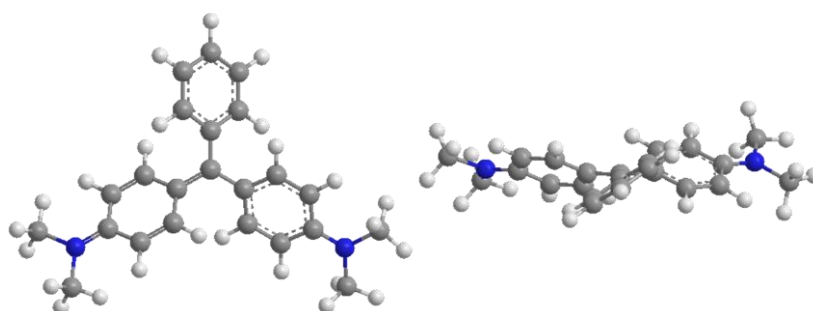


**Fig. S26** Chemical structure of MG, in which white, grey, and blue balls are hydrogen, carbon, and nitrogen atoms, respectively. Counterion is omitted.

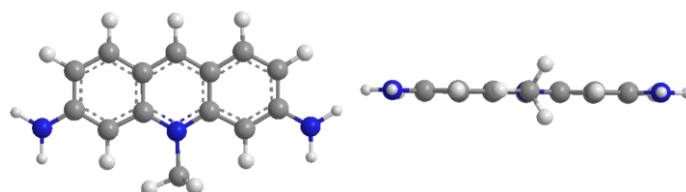


**Fig. S27** Chemical structure of AC, where white, grey, and blue balls are hydrogen, carbon, and nitrogen atoms, respectively. Counterion is omitted.

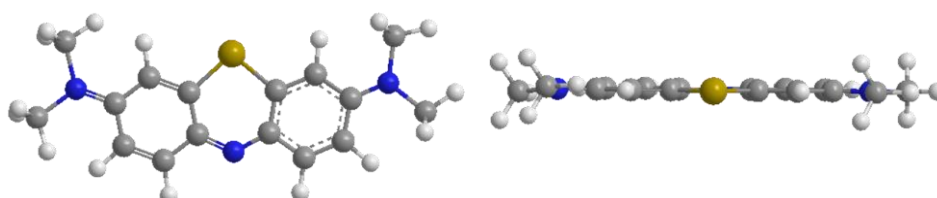


**Fig. S28** Chemical structure of MB, where white, grey, yellow and blue balls are hydrogen, carbon, sulphur and nitrogen atoms, respectively. Counterion is omitted.

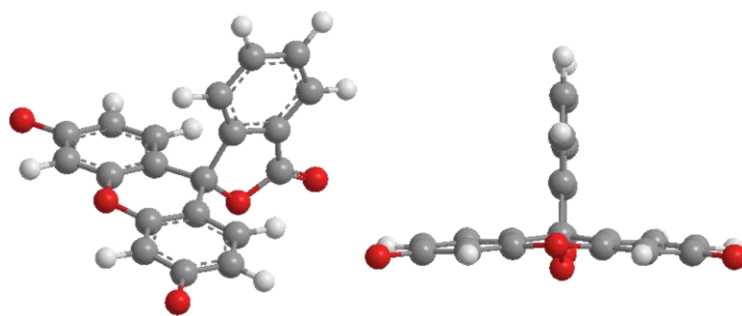


**Fig. S29** Chemical structure of FS, in which white, grey, and red balls are hydrogen, carbon, and oxygen atoms, respectively. Counterion is omitted.

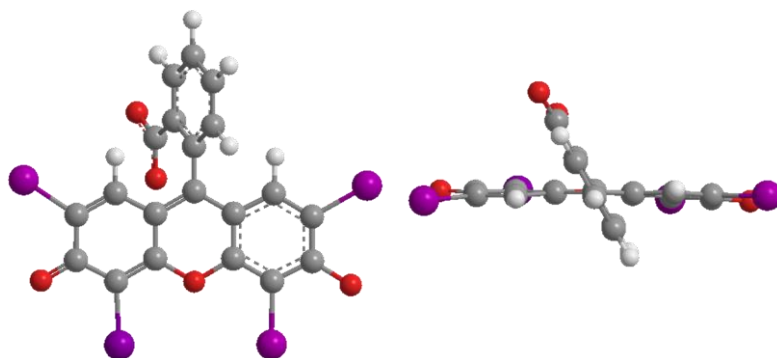


**Fig. S30** Chemical structure of EY, in which white, grey, purple and red balls are hydrogen, carbon, bromine and oxygen atoms, respectively. Counterion is omitted.

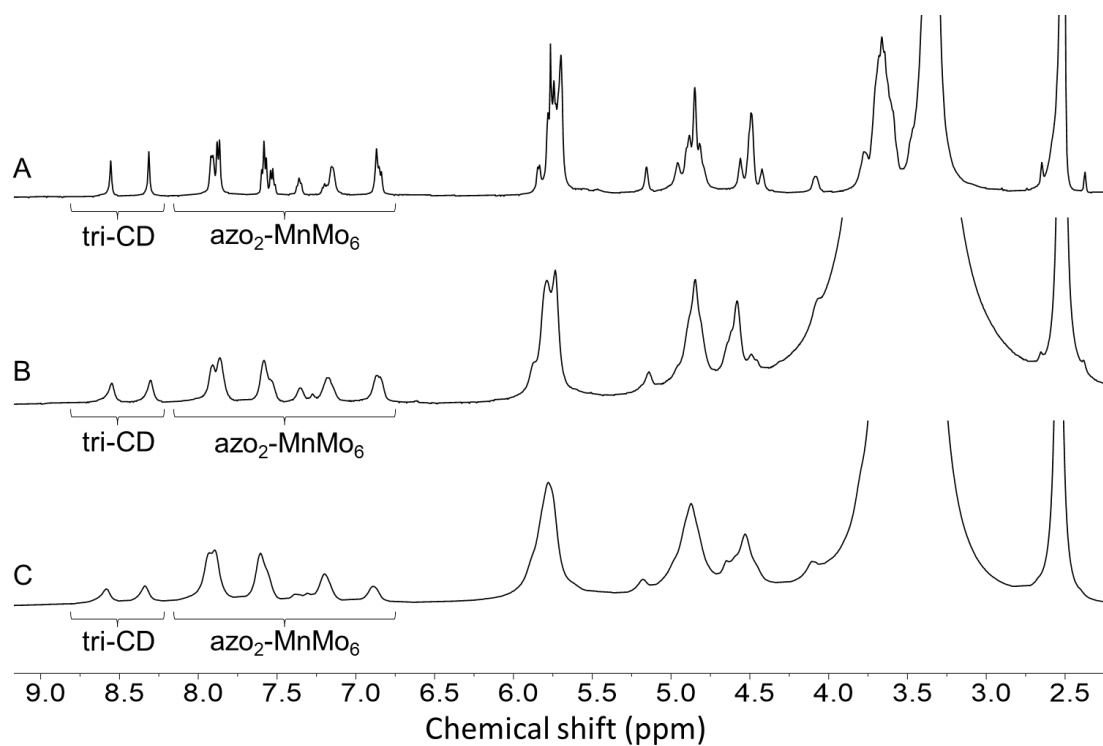


**Fig. S31** <sup>1</sup>H NMR spectra of (A) simple mixture of tri-CD and azo<sub>2</sub>-MnMo<sub>6</sub>, and the supramolecular assembly (B) before and (C) after degradation experiment in DMSO-*d*<sub>6</sub>.

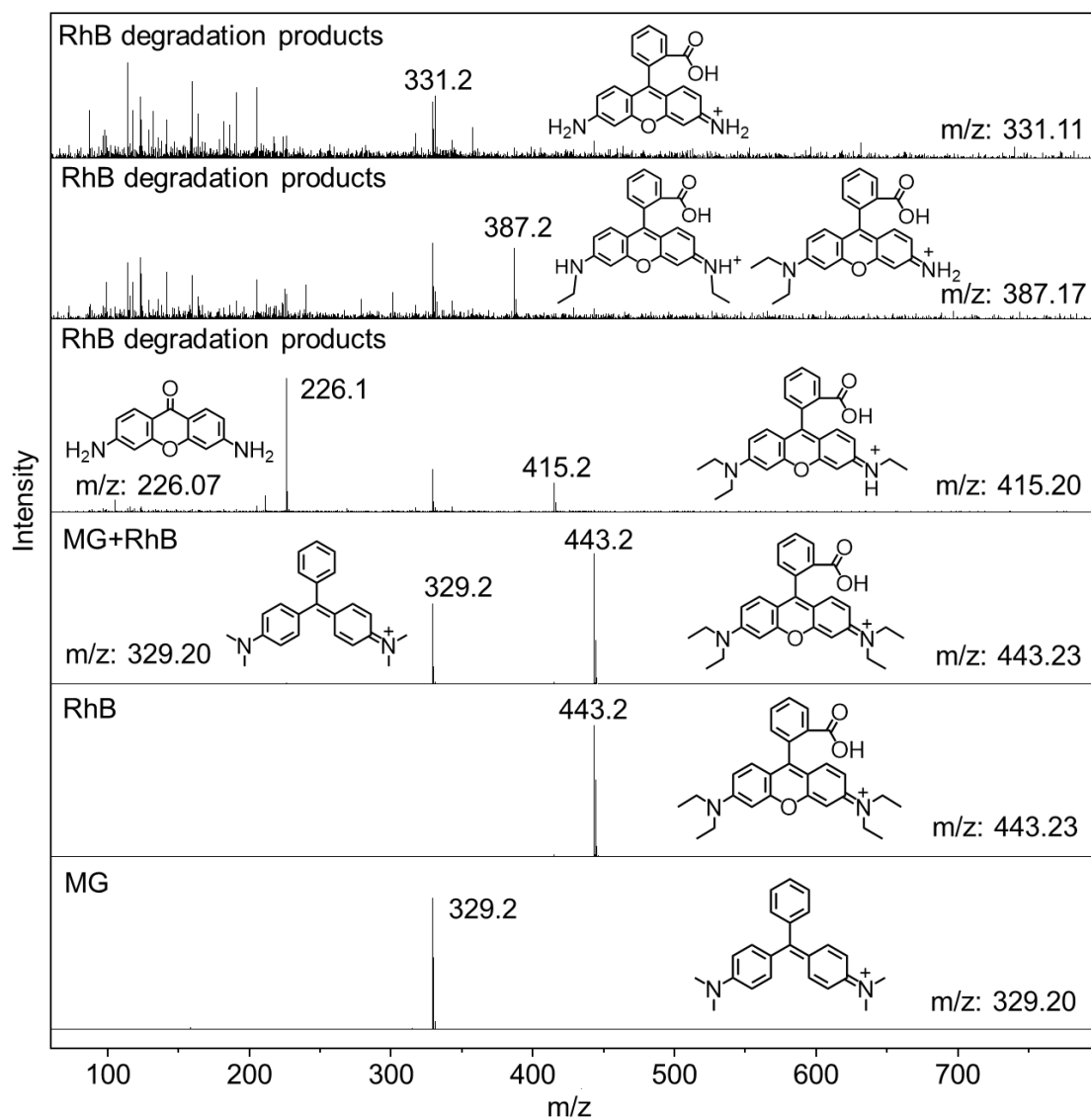


**Fig. S32** LC-MS spectra of RhB degradation products at different time and the corresponding initial mixture of RhB and MG, individual RhB and MG.

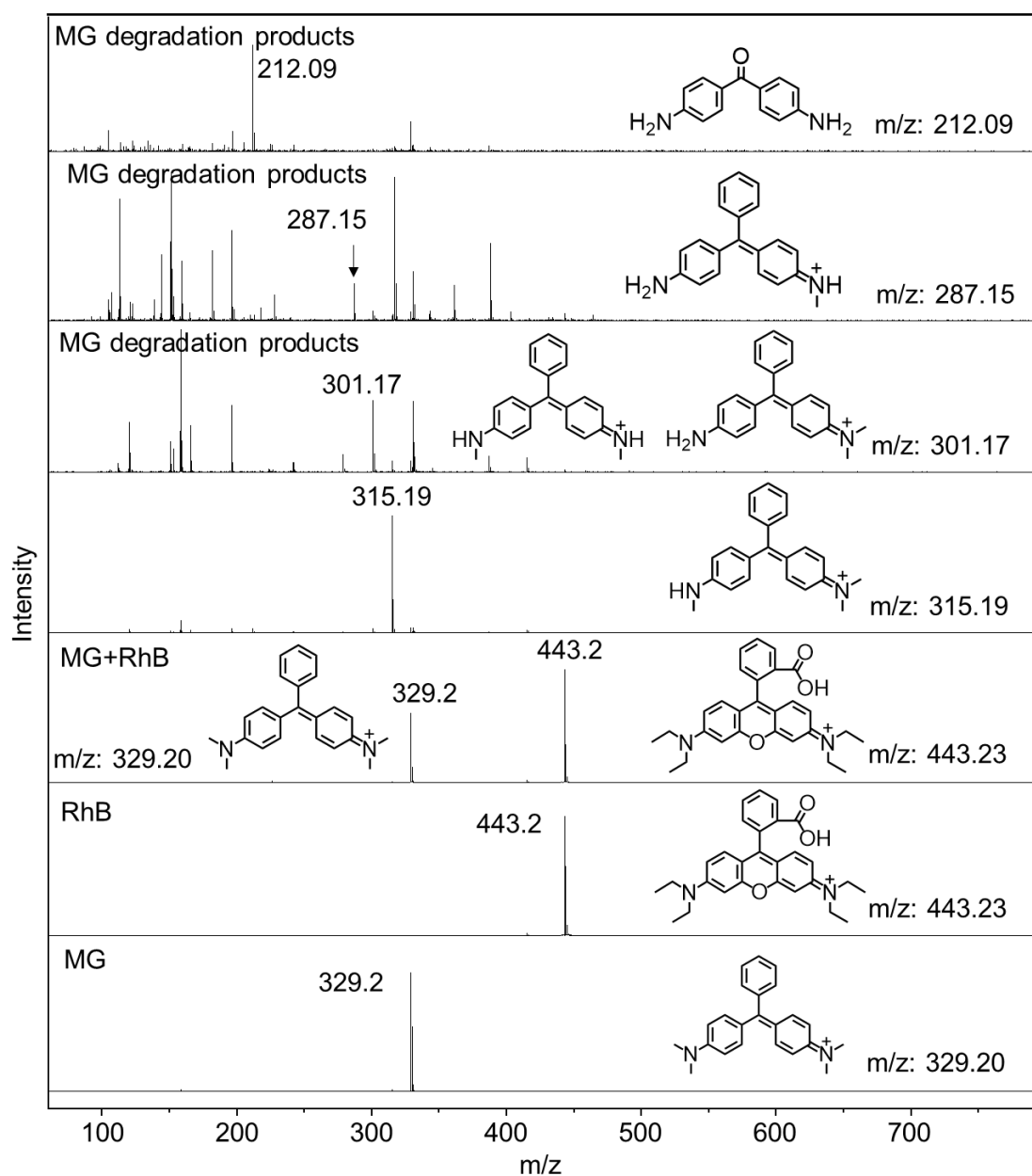


**Fig. S33** LC-MS spectra of MG degradation products at different time and the corresponding initial mixture of RhB and MG, individual RhB and MG.

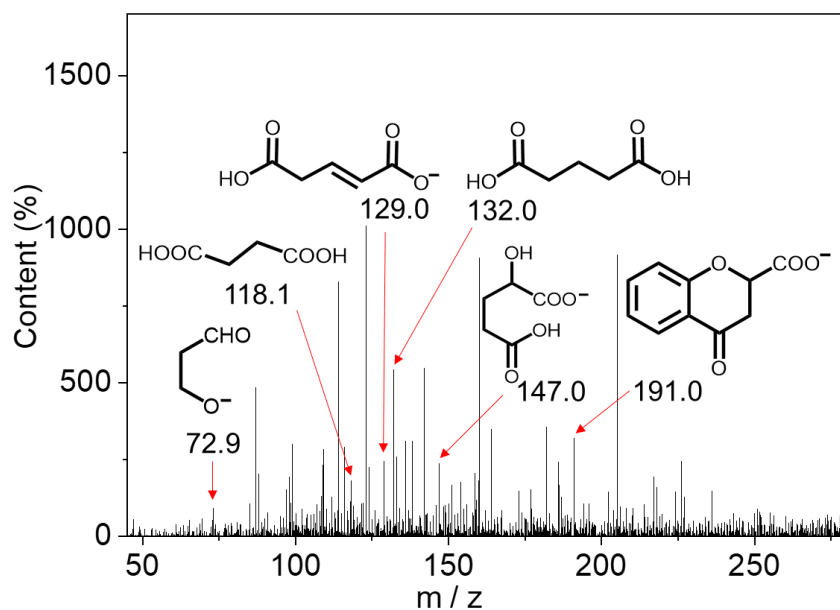


**Fig. S34** LC-MS spectrum of samll fragment of degradation products at final time.

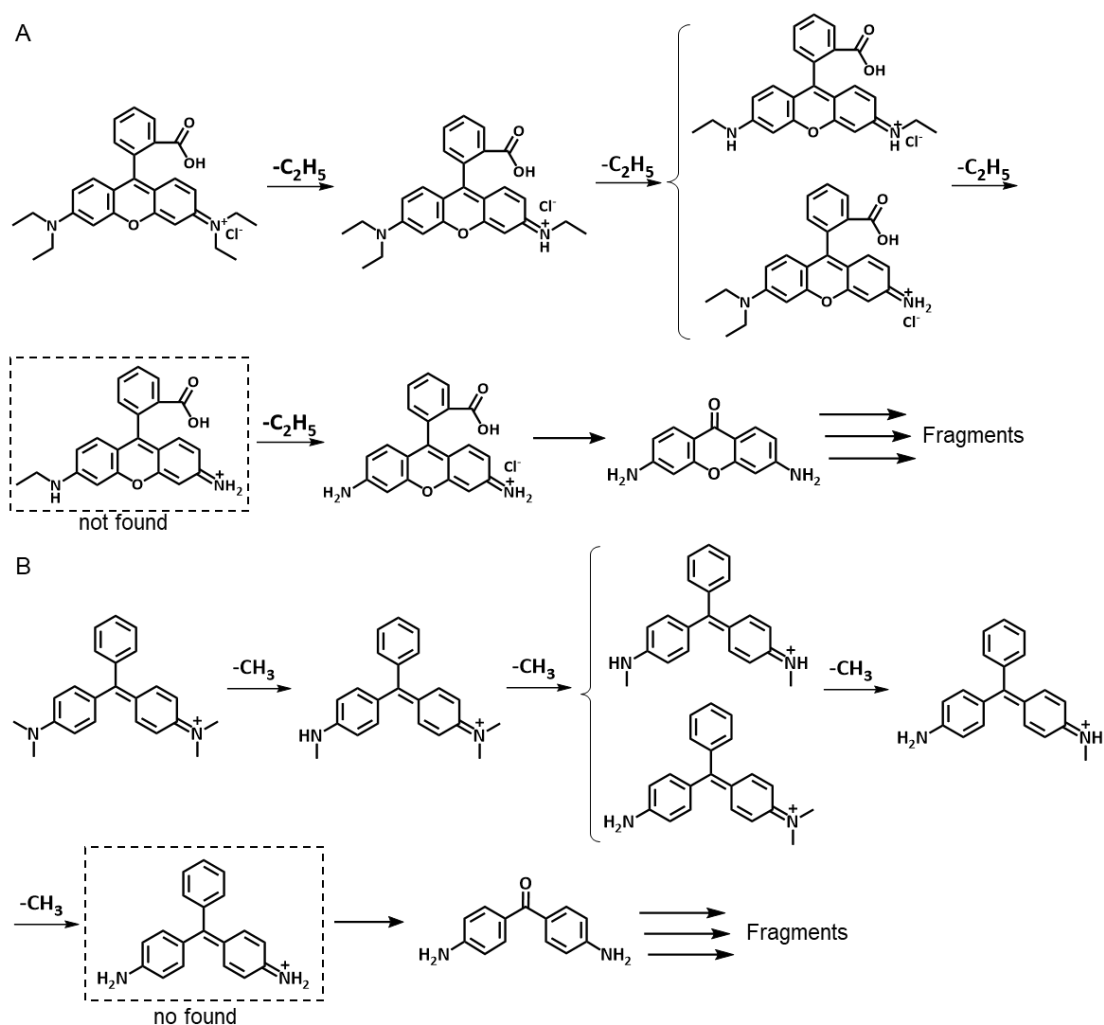


**Fig. S35** Proposed degradation mechanism of (A) RhB and (B) MG under the catalysis of supramolecular assembly in solutions.

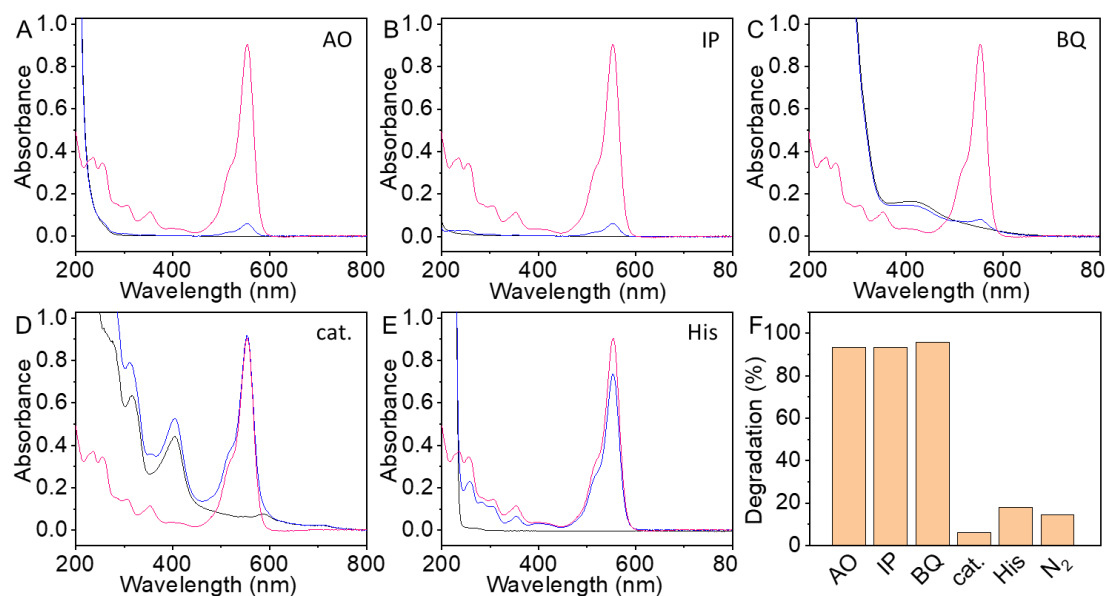


**Fig. S36** UV-vis spectra of RhB mixture with scavengers (A) Ammonium oxalate (AO), (B) isopropanol (IP), (C) benzoquinone (BQ), (D) catalase (cat.), and (E) L-histidine (HIS) after degradation for 66 h in dark place, in which red line denotes RhB before degradation, blue line means RhB encountering degradation, black line means the corresponding scavenger alone, and (F) columnar degradation values of scavenger.

## References

1. D. S. Philips, K. K. Kartha, A. T. Politi, T. Kruger, R. Q. Albuquerque and G. Fernandez, *Angew. Chem. Int. Ed.*, 2019, **58**, 4732–4736.
2. W. F. Jiang, Y. Liu, C. Y. Yu, S. L. Li, Y. J. Li and Y. F. Zhou, *Chem. Commun.*, 2016, **52**, 8223–8226.
3. L. Yue, H. Ai, Y. Yang, W. J. Lu and L. X. Wu, *Chem. Commun.*, 2013, **49**, 9770–9772.
4. B. Zhang, L. Yue, Y. Wang, Y. Yang and L. X. Wu, *Chem. Commun.*, 2014, **50**, 10823–10826.
5. B. Gao, G. X. Wang, B. Li and L. X. Wu, *ACS Omega*, 2020, **5**, 8127–8136.